Korean J. Chem. Eng., 33(12), 3381-3387 (2016)
DOI: 10.1007/s11814-016-0262-8

pISSN: 0256-1115
eISSN: 1975-7220

Design and analysis of a diesel processing unit for a molten carbonate fuel cell for auxiliary power unit applications

Agnesia Permatasari[*,], Peyman Fasahati[*], Jun-Hyung Ryu[***], and J. Jay Liu[*,†]**

*Brain Busan 21 Human Resource Education Team for Development of Green Energy Materials and Their Process, Pukyong National University, 365 Sinseon-ro, Nam-gu, Busan 48513, Korea
**Pulp and Paper Processing Technology, Institut Teknologi dan Sains Bandung, Jl. Ganesha Boulevard, Lot-A1 CBD Kota Deltamas, Tol Jakarta - Cikampek Km 37, Cikarang Pusat, Bekasi, Indonesia
***Department of Nuclear and Energy System, Dongguk University, Seokjang-dong, Gyeongju 38066, Korea
(*Received 31 May 2016 • accepted 9 September 2016*)

Abstract−Fuel cell-based auxiliary power units (APUs) are a promising technology for meeting global energy needs in an environmentally friendly way. This study uses diesel containing sulfur components such as dibenzothiophene (DBT) as a feed. The sulfur tolerance of molten carbonate fuel cell (MCFC) modules is not more than 0.5 ppm, as sulfur can poison the fuel cell and degrade the performance of the fuel cell module. The raw diesel feed in this study contains 10 ppm DBT, and its sulfur concentration should be reduced to 0.1 ppm. After desulfurization, the feed goes through several unit operations, including steam reforming, water-gas shift, and gas purification. Finally, hydrogen is fed to the fuel cell module, where it generates 500 kW of electrical energy. The entire process, with 52% and 89% fuel cell and overall system efficiencies, respectively, is rigorously simulated using Aspen HYSYS, and the results are input into a techno-economic analysis to calculate the minimum electricity selling price (MESP). The electricity cost for this MCFC-based APU was calculated as 1.57$/kWh. According to predictions, the cost reductions for fuel cell stacks will afford electricity selling prices of 1.51$/kWh in 2020 and 1.495$/kWh in 2030. Based on a sensitivity analysis, the diesel price and capital cost were found to have the strongest impact on the MESP.

Keywords: Fuel Cell, Auxiliary Power Unit, Diesel Processing, Desulfurization, Techno-economic Analysis

INTRODUCTION

Auxiliary power units (APUs) using fuel cells are attracting increasing attention as an environmentally friendly energy supply technology. APUs can provide electricity to many systems in ships beyond the main propulsion, such as lighting, plumbing, water pumping, fuel transfer, and navigation. Fuel cells can improve the efficiency of these auxiliary systems and conduct other functions in a much more environmentally friendly way than other technologies such as diesel engine-based APUs. According to Delphi Automotive Systems, solid oxide fuel cell (SOFC)-based APUs have higher efficiencies, lower fuel usages, and are better able to meet current emissions standards than diesel engines [1].

Fuel cells are low-polluting electrochemical devices that directly convert the chemical energy of hydrogen into electrical energy. Among the many types of fuel cells, we considered molten carbonate fuel cells (MCFCs). MCFCs can be operated at approximately 650 °C, which enables efficient recovery of residual pressure and waste heat via a gas turbine bottoming cycle and cogeneration [2,3]. For example, the operating temperature of phosphoric acid fuel cells (PAFCs) is lower than that of MCFCs. However, MCFCs have much higher operation efficiency (approximately 50-60%) than PAFCs (37-42%). When the waste heat is recovered, the overall fuel efficiency of MCFCs can be as high as 85% [4].

MCFC technology is considered as one of the most promising options for marine applications [5]. Technical feasibility of using fuel cells for ship propulsion and APUs has been demonstrated through successful applications for commercial, cruising, passengers and military navy ships, to list only a few, in North America and Europe.

High efficiency is one of the main reasons why MCFCs can offer significant cost reductions over PAFCs. Furthermore, MCFCs do not require an external reformer to convert more energy-dense fuels into hydrogen, unlike PAFCs and polymer electrolyte membrane fuel cells (PEMFCs), among other fuel cells. MCFCs are not prone to poisoning by carbon monoxide or carbon dioxide [6]. These fuel cells can even use carbon oxides as fuel, making them more attractive for fueling with coal-generated gases. Because MCFCs are more resistant to impurities than other fuel cells, coal could be internally reformed in MCFCs if they could be made resistant to impurities resulting from coal reforming, such as sulfur and particulates. Alternatively, because MCFCs require CO_2 be delivered to the cathode along with the oxidizer, MCFCs can be used to electrochemically separate carbon dioxide from the flue gas of other fossil fuel power plants for sequestration [7].

Fuel cells need primary resources as sources of hydrogen in the fuel stack to generate electricity. In this study, diesel was used as

†To whom correspondence should be addressed.
E-mail: jayliu@pknu.ac.kr
‡This article is dedicated to Prof. Ki-Pung Yoo on the occasion of his retirement from Sogang University.
Copyright by The Korean Institute of Chemical Engineers.

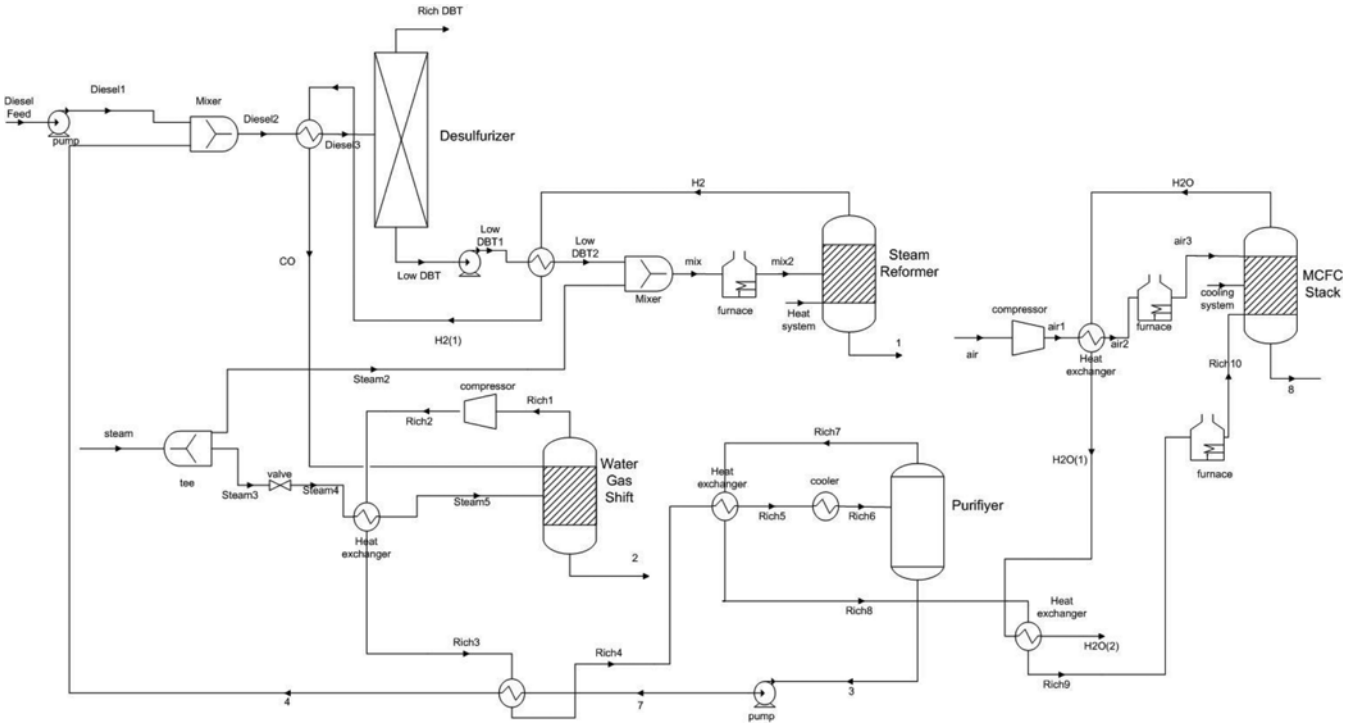

Fig. 1. Process flow diagram of an MCFC-based APU.

the primary resource. Diesel, which is mainly produced by the fractional distillation of crude oil, consists of a mixture of aliphatic hydrocarbons (C_9-C_{20}), aromatic hydrocarbons (including benzene and polycyclic aromatic hydrocarbons), and olefinic hydrocarbons. It also contains sulfur components such as dibenzothiophene (DBT), benzothiophene, and 4,6-methyldibenzothiophene. Hydrodesulfurization (HDS), oxidative desulfurization (ODS), oxidation-extraction desulfurization (OEDS), adsorptive desulfurization, and bio-desulfurization (BDS) are some of the technologies that are used, or have the potential to be used, to produce ultra-clean fuels able to meet standard emission regulations [6]. According to Korean Standard Specification for Diesel Fuel Oil (KS M 2610), upper specification limits of automotive diesel and marine diesel are 10 ppm and 500 ppm, respectively [8].

Above sulfur content level still can poison the catalyst in the steam reformer and fuel cell. Therefore, desulfurization in the fuel cell system is necessary to reduce the sulfur content of diesel. Via further desulfurization, the sulfur concentration of the diesel feed is reduced to enable safe entry to a steam reformer and prevent degradation of the fuel cell performance. Interestingly, desulfurization has often been ignored in many fuel cell application studies. For example, Delphi Automotive Systems decided to remove the desulfurization process in SOFC-based APUs because no sorbent performed well enough above 750 °C [1]. However, MCFCs have less restrictive high-temperature requirements.

Herein, all process units, including a desulfurization unit and an MCFC module, are rigorously simulated and analyzed. Although numerous works have simulated and analyzed fuel cell systems using diesel as a fuel, very few have included a desulfurization unit in the system, which is crucial in long-time applications of fuel cells. Therefore, the fuel cell system under consideration in this study is much more realistic and thus analysis of the system can provide useful insight into the system, such as economics of the system and its limiting factors. The rest of this paper is organized as follows: After system overview, detailed descriptions and conditions of unit processes and techno-economic analysis are given in Section 2. Simulation results and techno-economic analysis are assessed and discussed in Section 3. Summary and conclusion are given in Section 4.

METHODOLOGY

1. System Overview

The investigated MCFC system consists of the following sections: (1) desulfurization, (2) reaction and separation (steam reforming, water-gas shift reaction, and purification), and (3) MCFC module (see also Fig. 1).

Table 1. Chemical composition of diesel used

Component	Mole fraction
Dibenzothiophene (DBT)	0.0029
Naphthalene	0.0009
2-Methyl naphthalene	0.0009
n-C16	0.3162
n-C12	0.4154
n-C14	0.0010
t-Decalin	0.1294
Tert-butyl benzene	0.1337

Aspen HYSYS v8.6 is used for the modeling and simulation of a 500-kW APU including diesel fuel processing. Aspen HYSYS is extremely versatile and popular software used in the process industry for process modeling, conceptual design, and optimization. The chemical composition [9] of the diesel feed used in the simulation is summarized in Table 1. It is assumed that the sulfur compound in diesel is DBT, which can be found in the Aspen HYSYS component database.

2. Desulfurization Section

Among many types of desulfurization, we considered adsorptive desulfurization in the liquid phase. The most common adsorbents used in this type of process are activated carbon, zeolite, and silica gel. The sulfur components in the diesel feed are absorbed by the adsorbent, thereby separating them from the diesel feed. Based on this concept, the desulfurizer is simulated as a component splitter in Aspen HYSYS. The initial concentration of the sulfur compounds in diesel is 10 ppm. This concentration must be reduced to 0.1 ppm to avoid poisoning the catalyst in the steam reformer and the MCFC module. In this paper, the temperature used as an operating condition for desulfurization is 200 °C. The desulfurization unit is simulated as a single vessel, though there are two vessels in real situations: one for adsorption and one for regeneration. Both these functions are simulated in one device with a component splitter by adjusting the output pressure of the upper and bottom stage splitters with a 440-kPa inlet pressure [2,10]. It is assumed that there is a total 20% loss in diesel feed, including both adsorption and regeneration phases.

3. Reaction and Separation Section

Steam reforming is a commercial way of producing hydrogen from fossil fuel and is more efficient than partial oxidation (POX). The typical conditions of steam reforming are approximately 700-800 °C and 3 bar. Before steam reforming, gas phase diesel and steam are mixed, producing a gas mixture that can be safely heated in a steam reformer [11]. In the steam reformer, there is an external heat supply (low thermal heat) to keep the temperature constant.

After steam reforming, a water-gas shift is conducted to oxidize the carbon monoxide generated during steam reforming. The steam reforming [12,13] and water-gas shift [14-16] reactions are given in Eq. (1) and Eq. (2), respectively:

$$C_{12}H_{34}+12\ H_2O \rightarrow 25\ H_2+12\ CO \quad (1)$$

$$C_{12}H_{26}+16\ H_2O \rightarrow 33\ H_2+16\ CO$$
$$CO+H_2O \rightarrow CO_2+H_2. \quad (2)$$

In the purification section, a flash separator is used to separate gas products (mainly hydrogen) from liquid mixture (unreacted diesel). Our operation conditions for steam reforming, water-gas shift reaction, and separation were 720 °C and 300 kPa; 350 °C and 300 kPa; and 80 °C and 300 kPa, respectively [2].

Table 2. MCFC characteristics

Anode reaction	$H_2+CO_3^{2-} \rightarrow H_2O+CO_2+2e^-$
Cathode reaction	$CO_2+½\ O_2+2e^- \rightarrow CO_3^{2-}$
Overall reaction	$H_2+½\ O_2 \rightarrow H_2O$
Temperature (°C)	650
Pressure (kPa)	300
Cell voltage (Vcell) (V)	0.6

4. MCFC Section

The APU system considered in this study generates 500 kW of electrical energy. The operation temperature of the MCFC module is 650 °C [2]. The fuel cell characteristics are summarized in Table 2.

The utilization of hydrogen in the cell (η_{FP}) depends on the hydrogen that must be consumed to produce 500 kW of electricity. The H_2 consumption and utilization [14] are calculated according to Eqs. (3)-(6):

$$I = \frac{P}{V} \quad (3)$$

$$\text{mass of } H_2 \text{ consumed} = \frac{e \times I \times t}{F} \quad (4)$$

$$\text{mass flowrate } H_2 \text{ consumed} = \frac{\text{mass of } H_2 \text{ consumed (kg)}}{1\ \text{hr}} \quad (5)$$

$$\eta_{FP} = \frac{\text{mass flowrate } H_2 \text{ consumed}}{\text{mass flowrate inlet module}} \quad (6)$$

where P is the power (W), I is the electric current (A), V is the voltage (V), and t is the time (s). Furthermore, e is the gram equivalent weight, taken as 2, and F is the Faraday constant, 96,500 s A/mol.

The MCFC efficiency (η_{FC}) depends on the hydrogen utilization, which is defined as the percentage of hydrogen fuel reacted in the fuel cell. The stack voltage efficiency ($\eta_{stack\ voltage}$) and DC/AC conversion efficiency ($\eta_{AC/DC}$) are presented in Eq. (7)-(9):

$$\eta_{AC/DC}=0.98 \quad (7)$$

$$\eta_{stack\ voltage}=V_{cell} \times \eta_{FP} \quad (8)$$

$$\eta_{FC}=\eta_{stack\ voltage} \times \eta_{AC/DC} \quad (9)$$

where V_{cell} is the cell voltage in volts.

5. Techno-economical Analysis

Using the simulation results, the overall APU system cost is estimated to calculate the MESP. The economic parameters for the discounted cash flow analysis are shown in Table 3. The material and energy balance data from Aspen HYSYS simulation were used to

Table 3. Parameters used in the techno-economic analysis

Parameter	Value
Cost basis year	2015 dollars
Chemical engineering plant cost index (CEPCI)	579.5
Project life (years after startup)	10 years
Tax rate	35%
Annual interest rate	10%
Cost of raw material (C_{RM}) ($)	2,070,439
Cost of land	6% of Installed cost
Operating hours per period	8322 h/year
Construction period	2 years
Distribution of fixed capital investment:	
1. End of year one	60%
2. End of year two	40%

determine the number and the size of each equipment.

In estimating the capital cost, there are numerous important factors such as the fixed capital investment (FCI), working capital, utility cost, installed equipment cost, and manufacturing cost. The FCI was calculated by adding the direct costs such as materials, labor, and utilities, and indirect costs such as land taxes and insurance. The working capital represents the amount of capital required to start up the plant and finance the first few months of operation before the first process revenues are generated. The manufacturing cost, which represents the total costs of all resources consumed in making a product, can be determined from the FCI, cost of operating labor (C_{OL}), cost of utilities (C_{UT}), cost of water treatment (C_{WT}) and cost of raw materials (C_{RM}). The capital cost can be estimated in terms of the costs of the major plant equipment, which involves material and energy balances for each major piece of equipment, construction material selected, and the size/capacity set in the simulation [17].

As mentioned, the simulation includes two desulfurizers: one for sulfur adsorption and one for the regeneration process. Therefore, the installation cost of the desulfurization stage involves two desulfurizers. When estimating the MCFC cost, we used cost reduction projections by the National Renewable Energy Laboratory (NREL) to estimate future MCFC costs (see Fig. 2) [18], and calculated the MESP by setting the net present value (NPV) to zero.

A single-point sensitivity analysis was also performed on the constructed techno-economic model and parameters, including diesel price, capital cost, adsorbent price, total cost of utility (C_{UT}), and annual interest rate. Each parameter was changed to its maximum and minimum values while all other parameters were held constant at the same level.

RESULTS AND ANALYSIS

1. Simulation Results

Diesel was first fed to the desulfurization unit, where its sulfur compounds (DBT) were removed to avoid poisoning the catalyst in later processes. After desulfurization, the sulfur concentration of the diesel was below 0.1 ppm. The resulting diesel was then converted entirely into the gas phase and introduced into the steam reformer, where it was mixed with steam. The reforming was performed and produced hydrogen and carbon monoxide. To minimize carbon monoxide, a water-gas shift reaction was then conducted, in which carbon monoxide reacted with air and produced carbon dioxide and hydrogen. The hydrogen-rich gas was transported to the MCFC module to generate 500 kW of electricity. The simulation results for the individual streams are summarized in Table 4.

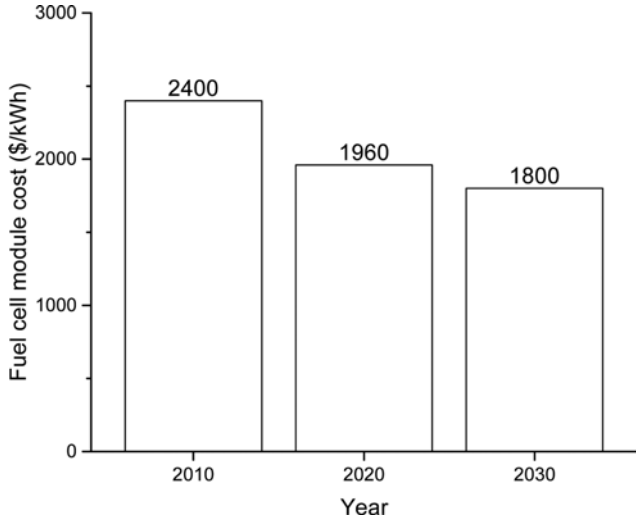

Fig. 2. Projected cost reduction of MCFC module [1].

Table 4. Equipment data for capital cost calculation [17]

Item	Cost US$	Year of quote
Desulfurizer	817,252	2015
Steam reformer	798,101	2015
Water gas shift	84,046	2015
Purifier	54,400	2015
Fuel cell module	1,200,000	2015

2. Desulfurization Section

Desulfurization was conducted in the liquid phase, in which 98% of DBT was separated from the diesel feed. It was then directed to the upper stage (rich DBT), where the DBT content of the feed was reduced from 0.0029 mol DBT/mol feed to 0.0001 mol DBT/mol feed. This value is within a safe range for the steam reformer and the fuel cell module. The upper-stage (regeneration process) pressure was 350 kPa [9,18], while the bottom-stage (adsorption process) pressure was 430 kPa [2,9]. Rich DBT was transported to the upper stage and separated from diesel, which was sent to the bottom output stage to be used in the next process. The desulfurization process resulted in a diesel feed with a 0.1 ppm sulfur concentration.

3. Reaction and Separation Section

There are two methods for converting hydrocarbons into hydrogen: partial oxidation and steam reforming. In partial oxidation, fuel is burned to produce carbon monoxide and hydrogen, which requires a high temperature (approximately 900 °C-1,500 °C). Meanwhile, in steam reforming, hydrocarbons are combined with steam via an endothermic reaction to produce hydrogen and other products. The operating temperature in the steam reforming process, approximately 700 °C-800 °C, is lower than that in the partial oxidation process. In this simulation, 720 °C was used as the process temperature. The steam reforming system is more efficient because the heat coming out of the process can be recycled. It also produces more hydrogen because hydrogen is obtained from the steam as well. The portion of the steam required for reacting $C_{16}H_{34}$ and $C_{12}H_{26}$ into a hydrogen product output is set so that the steam is only approximately 4% of the product of steam reforming [3] based on the reaction stoichiometry. If the steam output is more than 4%, then there will be excess steam in the output, which will affect the economics of the process. Hence, the input flow of steam entering the steam reformer is 234.2 kg/h. Conversion of hydrogen from $C_{16}H_{34}$ and $C_{12}H_{26}$ in the steam reformer is 75%, and the final mole fraction of hydrogen obtained in steam reforming is 0.6411.

In the next stage, the water-gas shift reaction occurs between carbon monoxide and water to produce additional hydrogen. In

Table 5. Variable operating cost [17]

Item	Cost
Diesel	0.76 $/kg
Adsorbent	3.8 $/kg
Cooling water	0.354 $/GJ
Low thermal source	12.33 $/GJ
Natural gas	11.1 $/GJ

this stage, the water-gas shift reactor is simulated as an equilibrium reactor. The conversion resulting from this process is 72%; thus, the mole fraction of produced hydrogen is increased to 0.6567. This result shows that CO was converted and additional hydrogen was produced. In addition to the water-gas shift reaction, the purification stage is also important for separating the remaining $C_{16}H_{34}$ and $C_{12}H_{26}$ for further recovery. As a result, both hydrocarbon outputs are 1% of the upper product. The mole fraction of hydrogen produced in this purification stage before entering the fuel stack module is 0.6623.

4. Molten Carbonate Fuel Cell Section

In the MCFC module, hydrogen from the steam reforming process was converted into 500 kW of electricity. The sulfur component of the diesel feed was decreased from 10 to 0.1 ppm in the desulfurization process as the sulfur tolerance of the MCFC module was at most 0.1 ppm. Thus, a 290 kg/h molar flow in the diesel feed was required for the generation of 500 kW of electricity in the MCFC module. The fuel cell utilization and fuel efficiency calculation are presented in Table 5. The fuel cell utilization shows how much hydrogen is consumed to generate 500 kW of electricity. In this simulation, a fuel-to-electricity efficiency of 52.33% can be achieved (Table 5). McPhail et al. [7] reported that the electrical efficiency of MCFC is 49%. The difference in efficiencies comes from the operation temperature of the MCFC: McPhail et al. operated their MCFC at approximately 500-550 °C, while the MCFC in this work was assumed to operate at 650 °C. The similar efficiencies validate the MCFC simulation in this work.

5. Techno-economic Analysis Results

The desulfurizer design [20,21] required in the techno-economic analysis is summarized in appendix A. The base cost for the fuel cell stack is 2,400 $/kW [22,23]. The total installed cost and fixed capital investment are listed in Table 6. From the techno-economic analysis, the MESP was computed as 1.57 $/kWh. Fig. 3 shows the breakdown of MESP breakdown for the base case (1.57 $/kWh). It

Table 6. Simulation results

Stream	Diesel feed	Air	Steam	Diesel3
Temperature (°C)	120	25	180	330
Pressure (kPa)	300	101.3	100	440
Molar flow (kg/h)	290	8655	2597	365.1
Stream	Mix2	CO	Rich6	Rich10
Temperature (°C)	720	349	80	650
Pressure (bar)	350	300	340	300
Molar flow (kg/h)	525.6	525.6	759.8	684.7

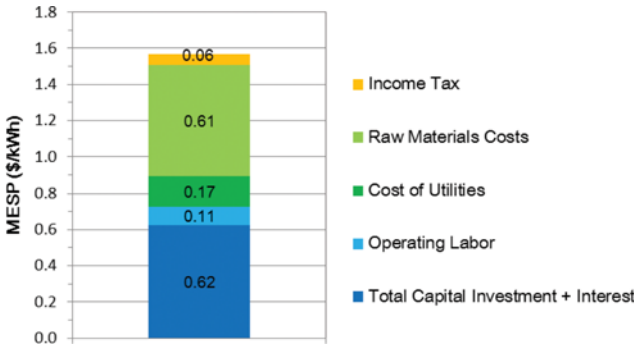

Fig. 3. MESP breakdown.

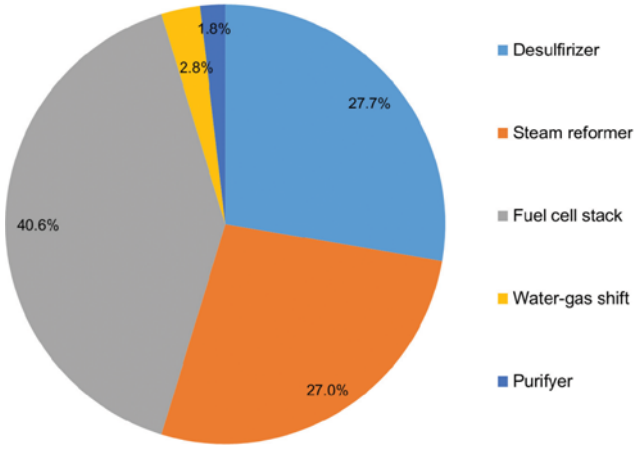

Fig. 4. Capital cost breakdown.

is clear from the figure that total capital investment and raw material costs take almost 80% of the MESP. As shown in Fig. 4, the fuel cell stack takes more than 40% of the equipment cost of major sections. Based on the predicted cost reductions of fuel cell stacks (see also Fig. 2), the electricity selling price will be 1.51 $/kWh in 2020 and 1.495 $/kWh in 2030.

6. Sensitivity Analysis

A single-point sensitivity analysis was performed on the techno-economic model and its parameters including diesel price, capital cost, adsorbent price, utility cost, and annual interest rate. The base-

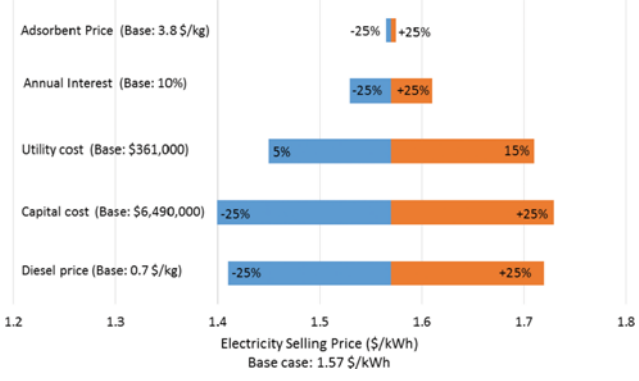

Fig. 5. Sensitivity analysis on MESP.

Table 7. Result of the MCFC section

Parameters	Value
I (ampere)	8.33×10^5
Mass of H_2 consumed (kg)	62.18
Mass flowrate H_2 consumed (kg/h)	69.86
η_{FP}	89%
η_{FC}	52.33%

Table 8. Total installed cost and fixed capital investment

	Cost
Total installed cost	$4,520,000
Cost of utility (C_{UT})	$361,000
Manufactured cost	$4,596,882
Working capital	$870,000
Fixed capital investment (FCI)	$6,490,000
Electricity selling price	1.57 $/ kWh

line for all variables is described above. Each variable was changed to its maximum and minimum values while all other parameters were held constant at the same level. We compared all parameters to identify those with the strongest impact on the MESP shown in Fig. 5. We changed the adsorbent price by up to ±25%. The electricity selling price was computed by varying the adsorbent price from 2.85 $/kg to 4.75 $/kg with annual interest rates of 5%, 10%, and 15%. For the capital cost and total C_{UT}, we again varied the values by up to ±25%. We compared the diesel prices over a range of ±25%. The electricity selling price was compared with diesel prices of 0.57 $/kg and 0.95 $/kg.

An adsorbent price of 3.8 $/kg yielded an electricity selling price of 1.38 $/kWh. However, changing this price by ±25% (from 2.85 $/kg to 4.75 $/kg) had little effect on the MESP.

The capital cost includes the price of the fuel cell stack. A capital cost of $7,050,000 gives an MESP of 1.57 $/kWh. When the capital cost was decreased by 25% (to $5,287,500), the electricity price decreased to 1.4 $/kWh. After a 25% increase (to $8,812,500), the MESP increased to 1.73 $/kWh.

An annual interest rate of 10% gives an MESP of 1.57 $/kWh. Changing the annual interest rate had little effect on the MESP: an annual interest rate of 5% gives an MESP of 1.45 $/kWh, whereas a 15% annual interest rate gives an MESP of 1.71 $/kWh.

Total C_{UT} of $563,000 gives an MESP of 1.57 $/kWh. However, if the utility cost is decreased by 25% (to $422,250), the electricity price becomes 1.53 $/kWh. Meanwhile, if it is increased by 25% (to $703,750), the MESP increases to 1.61 $/kWh.

A diesel price of 0.76 $/kg yielded an MESP of 1.57 $/kWh. Changing the annual interest rate had a significant effect on the MESP. When the adsorbent price was decreased by 25% (to 0.57 $/kg), the MESP decreased considerably to 1.41 $/kWh. Meanwhile, when the price was increased by 25% (to 0.95 $/kg), the MESP was 1.72 $/kWh.

Comparing the parameters, changes to the diesel price and capital cost have the strongest impact on the MESP. The MESP decreases from 1.57 $/kWh to 1.41 $/kWh if the diesel price decreases from 0.76 $/kg to 0.57 $/kg, and the MESP increases from 1.57 $/kWh to 1.72 $/kWh if the price increases from 0.76 $/kg to 0.95 $/kg. Furthermore, the MESP decreases from 1.57 $/kWh to 1.4 $/kWh if the capital cost (which includes the fuel cell stack price) decreases from $7,050,000 to $5,287,500, and the MESP increases from 1.57 $/kWh to 1.73 $/kWh if this price increases to 8,812,500.

CONCLUSIONS

The simulation predicted a hydrogen utilization (i.e., percentage of hydrogen fuel reacted in the fuel cell) of 89% and fuel cell stack efficiency of 52.33%. In the techno-economic analysis, the MESP for this MCFC-based APU was calculated as 1.57 $/kWh. The predicted cost reduction of fuel cell stacks gives an MESP of 1.51 $/kWh in 2020 and 1.495 $/kWh in 2030. Surprisingly, the cost reduction due to advances in future fuel cell technology alone cannot substantially lower the electricity price. This also indicates that significant MESP reduction can be achieved through technical advancements in the entire balance-of-plant (BOP). The sensitivity analysis showed that changes in the diesel price and capital cost have the strongest impact on the MESP. Because the sensitivity analysis also shows that the C_{UT} also affects the electricity selling price, more efficient heat integration is recommended.

Because of global warming, alternative energy sources are drawing increasing attention. The need for alternative energy sources cannot be enforced or welcomed without the development of their economically feasible operation strategy. Further research similar to this paper will be continued to accelerate the introduction of clean and sustainable energy sources.

ACKNOWLEDGEMENTS

This work was supported by the Pukyong National University Research Abroad Fund in 2014 (C-D-2014-0722).

REFERENCES

1. D. Hennessy and J. Banna, *Solid Oxide Fuel Cell Diesel Auxiliary Power Unit Demonstration*, FY 2012 Annual Progress Report, DOE Hydrogen and Fuel Cells Program (2012).
2. Ersoz, H. Olgun and S. Ozdogan, *J. Power Sour.*, **154**, 67 (2006).
3. P. Fornaserio and M. Graziani. *Renewable Resources and Renewable Energy: A Global Challenge*, Second Ed., CRC Press, New York (2011).
4. Y. Sanghai, *Techno Economic Analysis of Hydrogen Fuel Cell Used as An Electricity Storage Technology in a Wind Farm with High Amounts of Intermittent Energy*, Master's Thesis, University of Massachusetts, Amherst (2013).
5. C. S. Specchia, M. Antonini, G. Saracco and V. Specchia, *Int. J. Hydrogen Energy*, **33**, 3393 (2008).
6. H. P. Ho, W. H. Kim, S.-Y. Lee, H.-R. Son, N. H. Kim, J.-K. Kim, J.-Y. Park and H. C. Woo, *Clean Technol.*, **20**, 88 (2014).
7. A. Moreno, S. McPhail and R. Bove, *International status of molten carbonate fuel cell (MCFC) technology*, Joint Research Centre-Institute for Energy, JRC Scientific and Technical Report EUR 23373 (2008).

8. KS M 2610 Diesel Fuel Oil (2015).
9. X. L. Ma, L. Sun and C. Song, *Prepr. Pap.-Am. Chem. Soc., Div. Fuel Chem.*, **48**, 523 (2003).
10. G. Karagiannakis, P. Baltzopoulou, I. Dolios and A. G. Konstandopoulos, 9th PESXM: The Contribution of Chemical Engineering in Sustainable Development, May 23-25, Athens, Greece (2013).
11. B. Jurriaan, V. Erick, M. Sander ands B. Ruud, *J. Power Sour.*, **196**, 5928 (2011).
12. C. S. Specchia, M. Antonini, G. Saracco and V. Specchia, *J. Power Sour.*, **154**, 379 (2006).
13. B. Lindstro, J. A. J. Karlssonb, P. Ekdungea, L. De verdierb, B. Haggendalb, J. Dawodyb, M. Nilssonc and L. J. Petterssonc, *Int. J. Hydrogen Energy*, **34**, 3367 (2009).
14. Ersoz, H. Olgun and S. Ozdogan, *Energy*, **31**, 1490 (2006).
15. S. Ahmed, R. Kumar and M. Krumpelt, *Fuel Cells Bulletin*, **12**, 4 (1999).
16. V. C. Srivastava, *RSC Adv.*, **2**, 759 (2012).
17. T. Richard, R. C. Bailie, W. B. Whiting and J. A. Swaewitz, *Analysis, Syntesis, and Design of Chemical Processes*, 4th Ed., Prentice Hall, New Jersey (2012).
18. R. Robert and D. Wheeler, Molten Carbonate and Phosphoric Acid Stationary Fuel Cells: Overview and Gap Analysis, Technical Report No. NREL/TP-560-49072. National Renewable Energy Laboratory, Golden Colorado (2010).
19. G. Alptekin, A. Jayaraman, M. Dubovik, M. Schaefer, J. Monroe and K. Bradley, Desulfurization of Logistic Fuels for Fuel Cell APUs, TDA Research, Inc Wheat Ridge CO (2008). http://oai.dtic.mil/oai/oai?verb=getRecord&metadataPrefix=html&identifier=ADA504273.
20. R. Aris, *Ind. Eng. Chem. Fundamen.*, **4**, 227 (1965).
21. R. Aris, *The Mathematical Theory of Diffusion and Reaction in Permeable Catalyst: Vol. 1: The Theory of the Steady State*, Oxford University Press, New York (1975).
22. Ballard Power System Inc., Burnaby, British Columbia, Canada, http://ballard.com.
23. United States Environmental Protection Agency. *Renewable Energy Fact Sheet: Fuel Cells* (2013). http://nepis.epa.gov/Exe/ZyPURL.cgi?Dockey=P100IL86.txt.

APPENDIX A

Desulfurizer Design

1) Reaction rate constant (k)

$$\emptyset = \left[\frac{1}{\tanh 3\emptyset} - \frac{1}{3\emptyset}\right] = -\frac{R_{Ap} a^2}{D_A C_{As}} \quad \text{(A1)}$$

$$R_{Ap} = K\rho_p$$

$$C_{As} = \frac{P}{RT}$$

$$k = \left(\frac{3\emptyset}{R}\right)^2 D_A \quad \text{(A2)}$$

2) Volume of reactor (V_R)

$$V_R = -(1-\varepsilon_B)\left(\frac{RTN_{Af}}{\eta_{kP}}\right)\int_{N_{Af}}^{0.02N_{Af}} \frac{dN_A}{N_A} \quad \text{(A3)}$$

$$\eta = \frac{1}{\emptyset}\left(\frac{1}{\tan 3\emptyset} - \frac{1}{3\emptyset}\right)$$

$$\varepsilon_B = \frac{\rho_p}{\rho_b}$$

3) Required catalyst

$$W_c = \rho_b V_R \quad \text{(A4)}$$

K = pellet's production rate
ρ_p = density of pellet
ρ_b = density of bed
C_{As} = concentration of diesel (A) in terms of molar flows
R_{Ap} = production rate
D_A = diffusion coefficient of A
$\emptyset$ = thiele modulus
η = effectiveness factor
ε_B = bed porosity